ISSN : 0974 - 7540 Volume 2 Issue 2

Trade Science Inc.

Research & Reviews On Electrochemistry

Full Paper

RREC, 2(2), 2010 [95-102]

Electrocatalytic oxidation of phenol based on the plate like nano-$Ni(OH)_2$ /poly(thionine)/glass carbon electrode

Zhousheng Yang*, Fu Chen

College of Environmental Science and Engineering, Anhui Normal University, Wuhu, 241000, (P.R.CHINA)

E-mail : yzhoushe@mail.ahnu.edu.cn

Received: 27th October, 2010 ; Accepted: 6th November, 2010

ABSTRACT

In this work, plate like $Ni(OH)_2$ nanocrystals were synthesized with a simple hydrothermal synthesis method. The pretreated electrode was prepared by electropolymerizing thionine with Cyclic Voltammetry(CV) in phosphate buffer solution (PBS) containing thionine for 40 cycles. Then the next film was prepared by dropping nano-$Ni(OH)_2$ solution onto the poly(thionine)(PTH)/glass carbon electrode(GCE) surface. Additionally, the as-prepared nano-$Ni(OH)_2$/PTH/GCE showed a well electrocatalytic oxidation property towards phenol in 0.1 M PBS pH 7.0 via CV. Under the optimal conditions, the electrocatalytic response current of this sensor was proportional to the phenol concentration in the range of 0.08 μM ~ 180 μM with a detection limit down to 0.02 μM (S / N = 3). The phenol sensor exhibited low detection limit, fast response time, high selectivity. In consequence, the paper provided a quite effective and sensitive method for phenol detection.

KEYWORDS

Nano-$Ni(OH)_2$;
Poly(thionine);
Phenol;
Electroanalysis;
Electrocatalytic.

INTRODUCTION

Among organic pollutants, phenol and its derivative compounds were considered to be very toxic to humans as well as to the environment even at low concentrations[1,2]. Phenolic pollutants came from plastic, oil, food, coal, etc., which frequently discharged them in effluent wastes. Due to the carcinogenic risk for humans, the quantitative detection of phenolic compounds was highly relevant in environmental sciences[3]. Classical methods and techniques were used for determination of phenol quantification such as gas chromatography[4,5], liquid chromatography[6], liquid chromatography coupled with mass spectrometry[7,8], fluorescence[9], ultraviolet[10], capillary electrophoresis[11], and so on. Although the classical techniques were very powerful for monitoring toxic analysis, they were known to be expensive, time-consuming and require highly trained

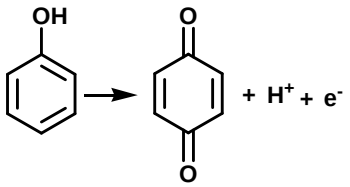

Scheme 1 : Reaction equation of phenol on the electrode

personnel[12]. Among these methods, electrochemical techniques appeared to be very promising because they ensured reasonably good analytical performance characteristics with essentially no need for sophisticated instrumentation. Furthermore, electrochemical detection was extremely attractive in terms of its potential for miniaturization[13,14].

Spataru et al.[15] reported a composite obtained by depositing platinum nanoparticles in a polytyramine (PTy) matrix, electrochemically formed on graphite substrate, was used as electrode material for the investigation of phenol oxidation. A rapid method for the determination of phenol within a concentration range of 0.3 ~10 mM was obtained. It should be noted that the porous structure of the polymeric matrix results in an increased susceptibility. Arecchi et al.[16] fabricated amperometric biosensor on a tyrosinase-modified electrode for the detection of phenolic compounds in food. The enzyme has been immobilized on a glassy carbon electrode covered by the polyamidic nanofibrous membrane prepared by electrospinning. Large specific surface area and high total porosity of nanofibrous membranes have enabled stable and highly sensitive performance for the sensor. These materials were also used as electrode modified materials for phenolic compounds electrooxidation. Thus, much work had been carried out in order to obtain and characterize the modified materials and it appeared that the materials could not only improve analytical performances (mainly due to higher active surface area) but also reduce the overpotential[17]. In particular, Ni(II) macrocycles have been shown to be good electrocatalysts for the oxidation of phenols and chlorophenols[18,19]. For instance, Obirai et al reported electropolymerization of the synthesized nickel tetra-4-(pyrrol-1-yl) phenoxyphthalocyanine. The poly-Ni(OH)TPhPyPc showed a better anti-fouling ability and stability in the presence of phenols and its derivatives. That could be attributed to the structure of the ring substituent on the phthalocyanine macrocycle and to the particular O–Ni–O bridged architecture of the nickel phthalocyanine film[20].

The chemical structure of thionine was a small planar molecule with two amino groups (-NH_2) symmetrically distributed on each side[21]. Both thionine monomer and the electrogenerated poly(thionine) had excellent electrocatalytic activity toward the redox of small molecular compounds. In addition, poly(thionine) as an excellent electron transfer mediator between the electrode and the redox centre had been widely used in many sensors[22,23]. Recently, the combination of inorganic nanomaterials and organic polymers to modified electrode was attractive for the purpose of creating high performance[24].

The present work reported on the electrochemical oxidation of phenol, which was oxidized by an interesting and relatively new approach on plate like nano-$Ni(OH)_2$/PTH/GCE. Direct electrochemical behavior of phenol on the modified GCE was explored in 0.1 M PBS pH 7.0 as the supporting electrolyte. The response dependences and amperometric characteristics including sensitivity, linear range, detection limit and stability of the electrodes were examined. The interrelated result was noteworthy because it provided us with improved performances for phenol anodic oxidation. Such a structured complex-based coating was at the origin of its particular electrocatalytic efficiency for the actions cited above.

EXPERIMENTAL

Reagent and materials

If not specified, all the chemicals were of analytical grade and used as received without any further purification. Phenol was purchased from Sinopharm Chemical Reagent Co., Ltd. Stock solution of phenol was prepared. The thionine solution (0.2673g, 0.02 M) was prepared with dissolving thionine in ethanol completely and then diluting with water. The supporting electrolyte was 0.1 M PBS. It was prepared by 0.1 M K_2HPO_4 and 0.1 M KH_2PO_4, and the various pH values from 5.0 to 10.0 were adjusted with 0.1 M H_3PO_4 and 0.1 M KOH. Moreover, doubly distilled water was used throughout the experiments.

Apparatus and measurements

All the electrochemical measurements including cyclic voltammetry and amperometric response (i-t) were carried out with CHI660-A electrochemical workstation (Chenhua Instruments Co., Shanghai, China). A conventional three-electrode system was employed. The working electrode was a bare glassy carbon electrode (GCE, Ø3.0 mm), poly(thionine)(PTH)/GCE, nano-

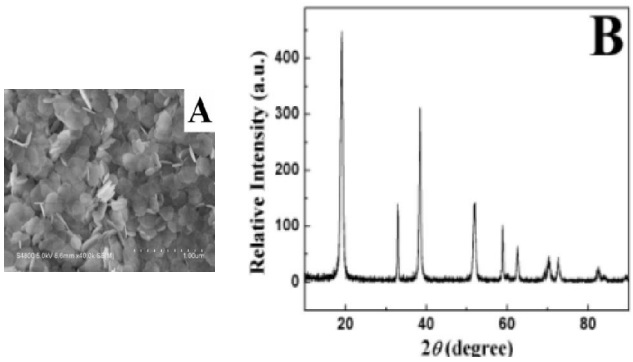

Figure 1 : SEM image (A:scale bar was 1 μm) and XRD pattern (B) of the as-prepared plate like Ni(OH)2 nanocrystals

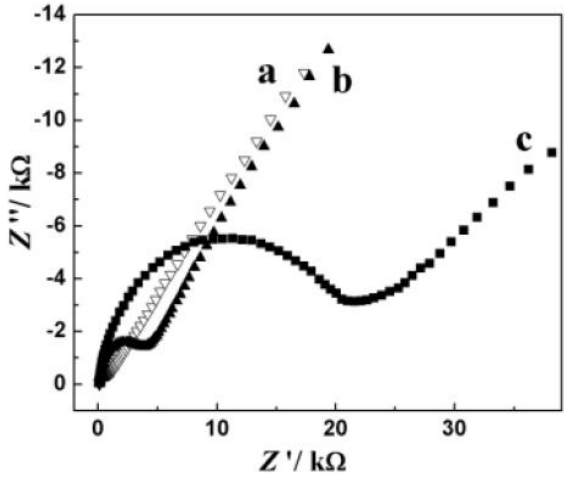

Figure 2 : Electrochemical impedance spectra of (a) bare GCE, (b) PTH/GCE, (c)nano-Ni(OH)2/PTH/GCE in 1 mM [Fe(CN)6] 3-/4-+1 M KCl

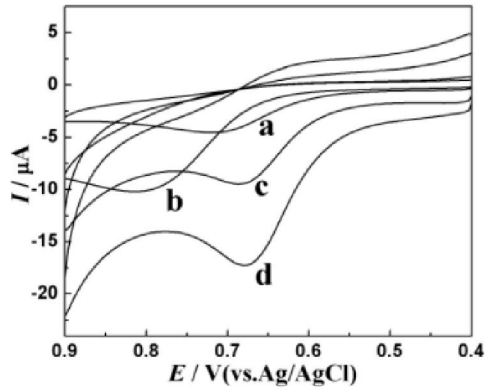

Figure 3 : Cyclic voltammograms of bare GCE (a) and first redox couple of nano-Ni(OH)2/GCE (b), PTH/GCE (c), nano-Ni(OH)2/PTH/GCE (d) in 0.1 M PBS pH7.0 containing 0.1 mM phenol. Scan rate: 0.10 V s-1

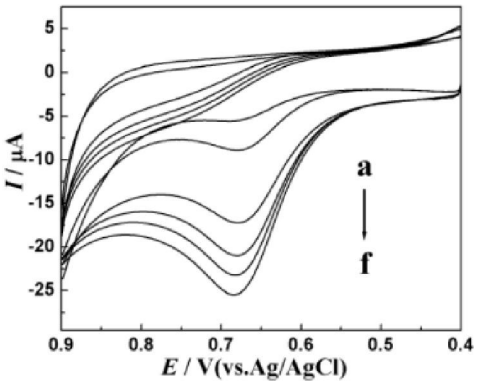

Figure 4 : Cyclic voltammetric curves at different concentrations of phenol in 0.1M PBS pH7.0: (a) 25 μM; (b) 50 μM; (c) 100 μM; (d) 130 μM; (e) 150 μM; (f) 170 μM

$Ni(OH)_2$/PTH/GCE, respectively. The Ag/AgCl（KCl, 3.0 M） electrode and a platinum wire were used as the reference electrode and the counter electrode, respectively. Scanning electron microscopy (SEM) was performed on S-4800 field emission scanning electron microanalyser (Hitachi, Japan). X-ray diffraction (XRD) was obtained with an X-ray diffractometer (Shimadzu, Japan) using a Cu K_α source (l = 0.154060 nm) at 40 kV, 30 mA in the range of $10°<2\theta<90°$ at a scan rate of 6.0° min^{-1}.

Preparation of the nano-$Ni(OH)_2$/PTH/GCE

The synthetic method of the nano-$Ni(OH)_2$ in this work was listed as follows: in the first place, 24.0 mL doubly distilled water and 24.0 mL absolute ethanol were poured into a beaker with stirring, 0.8838 g cetyltrimethylammonium bromide(CTAB), 0.3886 g $NiCl_2 \cdot 6H_2O$ and 0.134 g NaOH were orderly added into the above solution. Ten minutes afterwards it was tardily transfered into a 60 mL telflon - lined stainless steel autoclave. Completing all the above steps, it was necessary to make sure the autoclave was tightly sealed. Meanwhile, the temperature of autoclave stayed in 180°C for 24 h and then cooled to room temperature naturally. The precipitate was centrifuged and washed with doubly distilled water and absolute ethanol several times over and over, then dried in vacuum at 70°C for several hours.

Prior to electrooxidation process, the working GCE was mechanically polished with alumina powder (Al_2O_3, 0.05 μm) up to a mirror finish, thoroughly rinsed with doubly distilled water and sonicated in absolute ethanol and water (each for 5 min) and dried. Further the GCE was oxidized by performing 10 cycles in 0.1 M H_2SO_4 between 0 and 2.0 V at 0.10 V s^{-1} by CV[25]. The pretreated GCE was prepared by electropolymerizing thionine with CV between -0.50 and 0.50 V at 50 mV

Full Paper

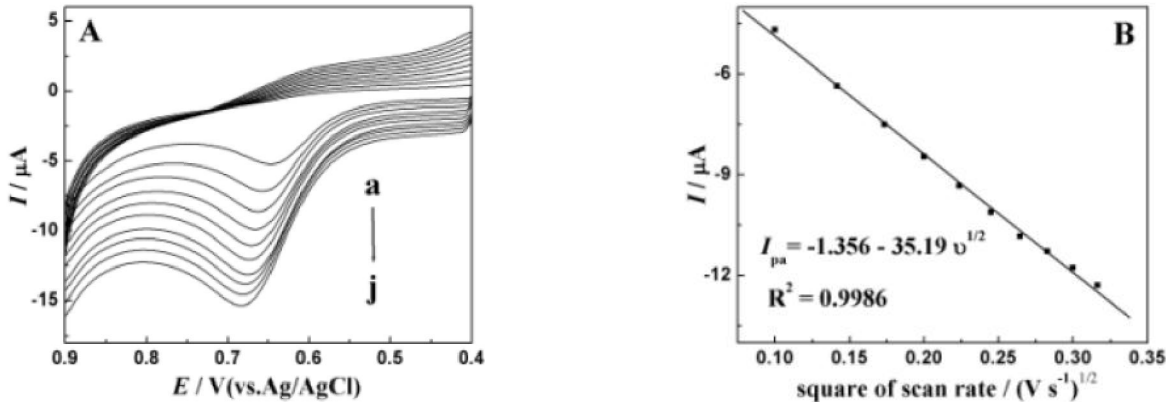

Figure 5 : Cyclic Voltammetric curves of nano-Ni(OH)2/PTH/GCE in 0.1 M PBS pH7.0 containing 0.1 mM phenol at different scan rates (Figure A), the scan rates from inner(a) to outer (j) were 0.01, 0.02, 0.03, 0.04, 0.05, 0.06, 0.07, 0.08, 0.09, 0.10 Vs-1, respectively. Figure B showed *I*pa vs. square of scan rate

s^{-1} in 5.0 mL 0.1 M PBS pH 6.0 containing 0.5 mM thionine for 40 cycles. The obtained PTH/GCE was washed with doubly distilled water and dried at room temperature. Next, the last film was prepared by dropping a certain volume (10 μL) of nano-$Ni(OH)_2$ (1.2 mg mL^{-1}) ethanol solution onto the PTH/GCE and then dried under ambient conditions. The nano-$Ni(OH)_2$/PTH/GCE was washed with doubly distilled water.

RESULTS AND DISCUSSION

Surface characterizations

Via scanning electron microscopy, the morphologies and structures of the surface film of the modified GCE was characterized. Figure 1A (scale bar was 1 μm) showed typical SEM images of the as-prepared nano-$Ni(OH)_2$. From the figure, it was clearly seen that the plate like product was evenly distributed. And the diameter of the nanoplate looked like about 200 nm. The nano-$Ni(OH)_2$ nanocrystals took on large specific surface area, very thin thickness and other advantages so as to improve sensitivity of the modified GCE. The crystallinity of the as-prepared $Ni(OH)_2$ nanoparticles were analysed via X-ray diffraction. Figure 1B showed the X-ray diffraction pattern (2θ scan) of the nanocrystals. By means of comparing with the standard graphs, the XRD pattern of these nanocrystals was consonant with the one of $Ni(OH)_2$. No other impurities were detected by XRD analysis, so verifying that the $Ni(OH)_2$ products were high pure phase.

A Nyquist diagram of electrochemical impedance spectrum was an effective way to measure the electron-transfer resistance. Figure 2 exhibited electrochemical impedance spectra of bare GCE, PTH/GCE, and the nano-$Ni(OH)_2$/PTH/GCE in 1.0 M KCl in the presence of 1.0 mM$[Fe(CN)_6]^{3-/4-}$ as the redox probe. As shown in figure 2, curve a was a nyquist plot of a bare GCE in 1.0 mM$[Fe(CN)_6]^{3-/4-}$. It exhibited an almost straight line, which implied an extremely low electron-transfer resistance to the redox probe. And then by electropolymerizing thionine on the pretreated GCE, the electron-transfer resistance increased (curve b, R_{et} = 4 kΩ), owing to the poly(thionine), the product of electropolymerization which hindered electron transfer on electrode surface. The next interfacial R_{et} (curve c, R_{et} = 21 kΩ) increased once again, which was due to the impediment of electron transfer in the presence of the nano-$Ni(OH)_2$ film. It indicated that the plate like $Ni(OH)_2$ nanocrystals were modified on the GCE successfully.

Electrochemical characteristics of the sensor

In order to explore the electrochemical behavior of phenol on the nano-$Ni(OH)_2$/PTH/GCE, the cyclic voltammetric experiments were performed in 0.1 M PBS pH 7.0 in the presence of 0.1 mM phenol with scanning potential from 0.40 to 0.90 V using different modified electrode as below, bare GCE, nano-$Ni(OH)_2$/GCE, PTH/GCE, and nano-$Ni(OH)_2$/PTH/GCE. The obtained cyclic voltammetric curves were shown in figure 3. As the figure seen, there was a weak electrochemical response to phenol at 0.72 V on the bare GCE. And on the nano-$Ni(OH)_2$/GCE, the anodic peak value of phenol was greater than the one on bare GCE

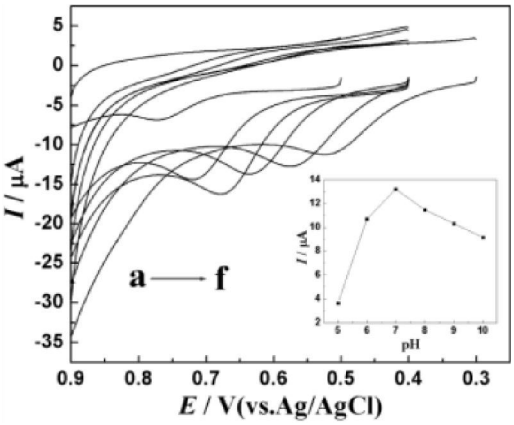

Figure 6 : Cyclic Voltammetric curves of nano-Ni(OH)2/PTH/GCE (vs.Ag/AgCl) to 0.1 mM phenol while using different pH (0.1 M PBS), including 5.0, 6.0, 7.0, 8.0, 9.0 and 10.0. Inset figure showed *I*pa vs. pH

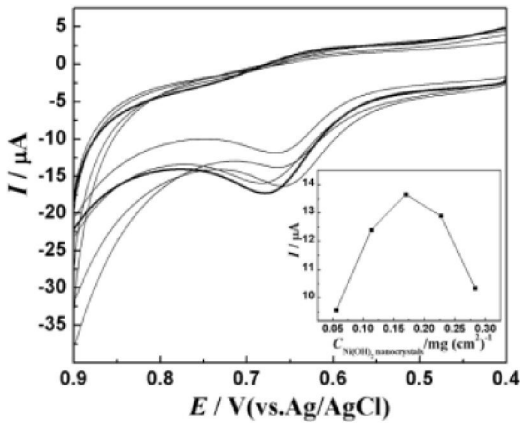

Figure 7 : Current response of nano-Ni(OH)2/PTH/GCE for 0.1 mM phenol inside the electrochemical reactor as various modification amount of Ni(OH)2 nanocrystals on the GCE per unit area; electrolyte: 0.1 M PBS pH7.0

under the same optimized conditions and the oxidation peak potential of phenol shifted a little towards positive potential. Moreover, the peak current on the PTH/GCE was further increased. While the surface of the above PTH/GCE was coated with nano-$Ni(OH)_2$ film, the peak current increased obviously. Furthermore, the oxidation peak potential shifted from 0.72 V at bare GCE to 0.68 V at as-prepared nano-$Ni(OH)_2$/PTH/GCE. And so the overpotential reduced. Accordingly we chose nano-$Ni(OH)_2$/PTH/GCE binding on the best electrocatalytic activity to phenol. As figure 4 displayed, the catalytic oxidation peak of phenol could be found in the potential range from 0.40 to 0.90 V in 5.0 mL supporting electrolyte solution containing phenol with increasing concentration. As can be seen, upon the addition of phenol, its anodic peak current of the modified GCE also increased.

Based on the obtained results and figures, we found that the poly(thionine) and synthetic nano-$Ni(OH)_2$ materials had not participated in the following reaction, the reaction of phenol on the nano-$Ni(OH)_2$/PTH/GCE could be described as follows. In the context of this work, the mechanism of phenol anodic oxidation had only a subsidiary connotation.

Figure 5 showed the cyclic voltammograms of nano-$Ni(OH)_2$/PTH/GCE in 5.0 mL 0.1 M PBS pH 7.0 solution. The figure 5A manifested the electrochemical behavior of the first electron reaction containing 0.1 mM phenol solution at various scan rates in the range from 0.01 to 0.10 V s^{-1}. The figure 5B emphasized the relationship between scan rates and the anodic peak current of phenol. The anodic peak current (I_{pa} / μA) was proportional to the square root of scan rate (υ/ V s^{-1}) (I_{pa} = -35.19$\upsilon^{1/2}$ -1.356, R^2 = 0.9986). The linearity dependence of the anodic peak current to the square root of the scan rate was observed over a narrow range of sweep rate. Such behaviors revealed that the anodic oxidation of phenol on the constructed electrode surface was diffusion controlled.

Optimization of the experiment conditions

The effect of pH on the oxidation of phenol was studied by CV using nano-$Ni(OH)_2$/PTH/GCE. Figure 6 presented Cyclic Voltammetric curves for the measurement of 0.1 mM phenol with various pH that were adjusted using 0.1 M PBS in the range of 5.0 ~ 10.0. As the figure shown, with pH rising, the anodic peak current value was greater. As up to a certain degree, the peak current achieved the best value. Subsequently, it came to a gradual decrease. Besides, it was observed that the peak current response was the best while adopting pH 7.0, roughly the physiological pH. Under the higher acidity, the nano-$Ni(OH)_2$ particles could not exist steadily in the acidic medium, resulting in anodic peak current of phenol decreasing. As the alkalinity was stronger, the PTH was unsteady because the NH_3^+ in the structure could convert to NH_2 group, and the structure of poly (thionine) could be destroyed probably. The anodic peak current of phenol also decreased. Accordingly, during this experiment we chose 0.1 M PBS pH 7.0 as the supporting electrolyte.

Film thickness of the modified electrode might also

Full Paper

TABLE 1 : Comparison of performances of proposed sensor for phenol detection with other methods

Method	Linear range(μM)	Detection limit(μM)	Sensitivity	Reference
Immobilizing Hemoglobin (Hb) in a sol–gel matrix onto a carbon electrode	5~50	0.8	365μA mM^{-1}	[1]
Electropolymerized PTS-doped polypyrrole film	3.3~220	0.8	17.1 μA mM^{-1}	[26]
Hybrid titania sol–gel matrix	0.025~6	0.01	1605 μA mM^{-1}	[27]
Colloidal gold-modified carbon paste electrode	4~48	0.0061	23 μA mM^{-1}	[28]
Gold nanoparticlesmodified GC electrodes	1~40	0.21	82 μA mM^{-1}	[29]
Nano-ZnO/chitosan	0.15~65	0.05	182 μA mM^{-1}	[30]
ZnO nanorod microarrays on the nanocrystalline diamond electrode	1~150	0.2	287.1 μA mM^{-1} $cm^{?2}$	[31]
nano-Ni(OH)2/PTH/GCE	0.08~180	0.02	132 μA mM^{-1}	this work

affect the performance of the phenol electrochemical sensor. Figure 7 presented the peak current response difference among various nano-$Ni(OH)_2$ film thickness to 0.1 mM phenol. We made up a series of concentrations including 0.4, 0.8, 1.2, 1.6, 2.0 mg mL^{-1} nano-$Ni(OH)_2$ ethanol solution. The diameter of the glassy carbon electrode was 3 mm. Thus, we calculated the amount of nano-$Ni(OH)_2$ on the electrode per unit area, which was respectively 0.056, 0.113, 0.170, 0.227, 0.283 mg $(cm^2)^{-1}$. From the figure, we could see the anodic peak current became greater at the outset and after dropping off with the film thickness increasing. The phenomenon manifested that the electric current response was optimal as we employed 1.2 mg mL^{-1} nano-$Ni(OH)_2$ solution. The mass transport and charge transfer rate of the sensor might decrease when the nano-$Ni(OH)_2$ film was too thick.

Depending on all above studies, we obtained proper experimental conditions.

Amperometric response to phenol and the calibration curve

To shed more light on the roles of poly(thionine) and $Ni(OH)_2$ nanocrystals, the amperometric response of nano-$Ni(OH)_2$/PTH/GCE upon adding phenol little by little was tested at the applied potential 0.68 V in 0.1 M PBS pH 7.0 with continuous stirring under the optimal conditions. The fabricated sensor yielded a rapid and sensitive response to each injection of phenol (within 3 s). As was exhibited in figure 8, well responses were observed during the successive addition of 0.08, 0.2, 0.6 and 1 μM phenol, respectively, the phenomenon demonstrated an effective catalytic property of nano-$Ni(OH)_2$/PTH/GCE. The addition of phenol was marked by arrows at the concentrations mentioned. The plot of I_{pa} versus C_{phenol} (inset, Figure 8) depicted a linear relationship over the range from 0.08 μM to 180 μM. The regression equation was Y(μA) = - 0.105 - 0.132X(μM) with the correlation coefficient being 0.997, and the detection limit was computed to be 0.02 μM at a signal-to-noise ratio of 3. The sensitivity was calculated as 132 μA mM^{-1} at a potential of 0.68 V. Therefore, this sensor was of high sensitivity. In addition, this electrochemical sensor has displayed both catalytic performance and high sensitivity due to the synergy of some active groups resulting from oxidation process on electrode surface, good conductive nature of electrochemical poly(thionine) and the large surface area of the $Ni(OH)_2$ plate like nanostructure. Varied methods regarding phenol detection could result in different effects. TABLE 1 summarized the performance of the proposed sensor for phenol detection based on different methods. By this token, our work was potential.

Anti- interference ability of the sensor

In real samples, some co-existing electroactive species might affect the sensor response. And so the possible interferences such as catechol, hydroquinone and o-nitrophenol on the response current to phenol at the potential of 0.68 V were studied at the developed sensor. As illustrated in figure 9, when 100 μM catechol, 100 μM hydroquinone and 100 μM o-nitrophenol were orderly added in 0.1 M PBS, no significant interference was found at this potential. Results illuminated that those compounds did not interfere with the calibration assay. It was clear from above results that the as-prepared sensor could offer high selectivity.

Stability and recovery test

The stability of the sensor was investigated in the

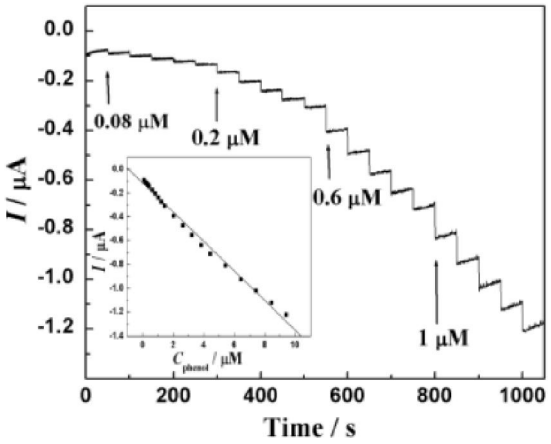

Figure 8 : Amperometric current–time curves for phenol oxidation at the plate like nano-Ni(OH)2/PTH/GCE. Electrodes were held at an applied potential of 0.68 V (vs. Ag/AgCl) and rotated at 1000 rpm in a 5mL 0.1 M PBS pH7.0. The current–time curves for adding 0.08, 0.2, 0.6, 1 μM of phenol. Inset figure showed *I*pa vs.*C*phenol

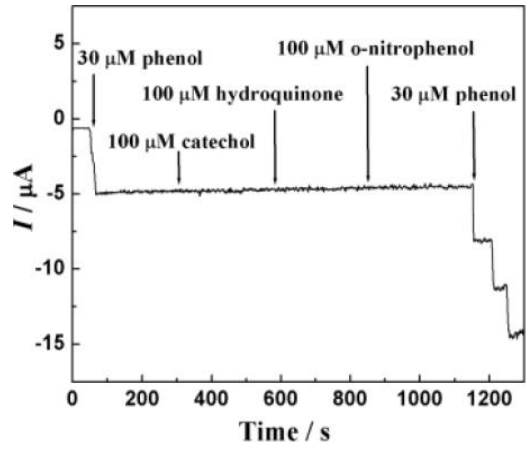

Figure 9 : Effects of catechol, hydroquinone and o-nitrophenol interferences on the amperometric response of the nano-Ni(OH)2/PTH/GCE to phenol in 5 mL 0.1 M PBS pH7.0. Operating potential: 0.68 V

working solution containing 0.1 mM phenol. When the sensor was stored in a refrigerator at 4°C for four days, no obvious decrease of the response current was observed. Then after the storage of three weeks at 4°C, the sensor retains 85.3% of its initial current response. These results were satisfactory with the decent stability of the sensor.

For the sake of verifying the applicability of the nano-$Ni(OH)_2$/PTH/GCE for environment analysis. The recovery of phenol in water sample was performed on the sensor utilizing standard addition method. All the measurements were carried out three times. In the best conditions, the sensor was also tested by the phenol

TABLE 2 : Recovery of phenol sensor

Phenol added (10^{-4} M)	Found[a] (10^{-4} M)	Recovery (%)
0.01	0.0107	107%
0.05	0.049	98%
0.1	0.093	93%
0.5	0.52	104%
1	0.96	96%

[a]**Average of three detections**

recovery experiments in the water samples, which showed satisfactory results, with average recoveries from 93 to 107 %, as presented in TABLE 2, suggesting that it was feasible to apply the proposed method to quantitatively detection of the certain concentration range of phenol in water sample.

CONCLUSIONS

A nano-$Ni(OH)_2$/PTH/GCE was fabricated, and was applied to detect the concentration of phenol. The as-prepared sensor had good catalytic ability for the oxidation of phenol, which greatly facilitated the electron exchange between phenol and GCE owing to large surface-to-volume ratio of plate like $Ni(OH)_2$ nanomaterials chiefly and high efficient electron transport property of poly(thionine). Under the optimized conditions, the sensor with multilayers demonstrated success for the detection of phenol with high analytical sensitivity and fast response. The electrocatalytic response current of the sensor was proportional to phenol concentration in the range of 0.08 μM ~ 180 μM with a detection limit down to 0.02 μM (S / N = 3). The overpotential of the proposed electrode for the oxidation of phenol was lower than the one of bare GCE. In addition, catechol and hydroquinone exhibited no interference to the detection. The nano-$Ni(OH)_2$/PTH/GCE promised a vast range of application for the detection of phenol contaminant from wastewater.

ACKNOWLEDGEMENTS

We thank the National Natural Science Foundation of China (Grant No. 20775002) for financial support. The work was supported by Program for Innovative Research Team in Anhui Normal University.

Full Paper

REFERENCES

[1] A.K.M.Kafi, D.Y.Lee, S.H.Park, Y.S.Kwon; Thin Solid Films, **516**, 2816 **(2008)**.
[2] P.Bankovic, Z.Mojovic, A.Milutinovic-Nikolic, N.Jovic-Jovicic, S.Marinovic, D.Jovanovic; Applied Clay Science, **49**, 84 **(2010)**.
[3] L.Fernandez, C.Borras, H.Carrero; Electrochim. Acta, **52**, 872 **(2006)**.
[4] S.D.Richardson; Anal.Chem., **74**, 2719 **(2002)**.
[5] R.B.Geerdink, W.M.A.Niessen, U.A.T.Brinkman; J.Chromatogr.A, **975**, 65 **(2002)**.
[6] T.A.Berger, J.F.Deye; J.Chromatogr.Sci., **29**, 54 **(1991)**.
[7] T.Benijts, W.Lambert, A.De Leenheer; Anal.Chem., **76**, 704 **(2004)**.
[8] N.Yoshioka, Y.Akiyama, K.Teranishi; J.Chromatogr.A, **1022**, 145 **(2004)**.
[9] B.Saad, N.H.Haniff, M.I.Saleh, N.H.Hashim, A.Abu, N.Ali; Food Chem., **84**, 313 **(2004)**.
[10] R.D.Thompson; J.AOAC Int., **84**, 815 **(2001)**.
[11] C.Brage, K.Sjostrom; J.Chromatogr., **538**, 303 **(1991)**.
[12] Y.F.Li, Z.M.Liu, Y.L.Liu, Y.H.Yang, G.L.Shen, R.Q.Yu; Anal.Biochem., **349**, 33 **(2006)**.
[13] H.Xue, Z.Shen; Talanta, **57**, 289 **(2002)**.
[14] J.Zhang, J.P.Lei, Y.Y.Liu, J.W.Zhao, H.X.Ju; Biosens.Bioelectron., **24**, 1858 **(2009)**.
[15] T.Spataru, N.Spataru; J.Hazard.Mater., **180**, 777 **(2010)**.
[16] A.Arecchi, M.Scampicchio, S.Drusch, S.Mannino; Anal.Chim.Acta, **659**, 133 **(2010)**.
[17] A.K.M.Kafi, A.Chen; Talanta, **79**, 97 **(2009)**.
[18] M.Manriquez, J.L.Bravo, S.Gutierrez-Grandos, S.S.Succar, C.Bied-Charreton, A.A.Ordaz, F.Bedioui; Anal.Chim.Acta, **378**, 159 **(1999)**.
[19] M.S.Ureta-Zanartu, C.Berrios, J.Pavez, J.Zagal, C.Gutierrez, J.F.Marco; J.Electroanal.Chem, **553**, 147 **(2003)**.
[20] J.Obirai, F.Bedioui, T.Nyokong; J. Electroanal. Chem., **576**, 323 **(2005)**.
[21] Q.W.Li, J.Zhang, H.Yan, M.S.He, Z.F.Liu; Carbon, **42**, 287 **(2004)**.
[22] Q.Gao, X.Q.Cui, F.Yang, Y.Ma, X.R.Yang; Biosens.Bioelectron, **19**, 277 **(2003)**.
[23] R.Yang, C.M.Ruan, W.L.Dai, J.Q.Deng, J.L.Kong; Electrochim.Acta, **44**, 1585 **(1999)**.
[24] Z.J.Yin, J.J.Wu, Z.S.Yang; Microchim.Acta, **170**, 307 **(2010)**.
[25] S.Thiagarajan, T.H.Tsai, S.M.Chen; Biosens.Bioelectron, **24**, 2712 **(2009)**.
[26] R.Rajesh, W.Takashima, K.Kaneto; React.Funct. Polym., **59**, 163 **(2004)**.
[27] T.Zhang, B.Tian, J.Kong, P.Yang, B.Liu; Anal.Chim.Acta, **489**,199 **(2003)**.
[28] S.Liu, J.Yu, H.Ju; J.Electroanal.Chem., **540**, 61 **(2003)**.
[29] V.Carralero Sanz, M.Luz Mena, A.Gonzalez-Cortés, P.Yanez-Sedeno, J.M.Pingarron; Anal.Chim.Acta, **528**, 1 **(2005)**.
[30] Y.F.Li, Z.M.Liu, Y.L.Liu, Y.H.Yang, G.L.Shen, R.Q.Yu; Anal.Biochem., **349**, 33 **(2006)**.
[31] J.W.Zhao, D.H.Wu, J.F.Zhi; Bioelectrochemistry, **75**, 44 **(2009)**.